

## Supporting Information

### **Stretchable and recyclable liquid metal droplets embedded elastomer composite with high mechanically sensitive conductivity**

**Xiaokang He<sup>1</sup>, Jianpeng Wu<sup>1</sup>, Shouhu Xuan<sup>1\*</sup>, Shuaishuai Sun<sup>2</sup>, Xinglong Gong<sup>1\*</sup>**

*<sup>1</sup>CAS Key Laboratory of Mechanical Behavior and Design of Materials, Department of Modern Mechanics, University of Science and Technology of China, Hefei 230027, China*

*<sup>2</sup>CAS Key Laboratory of Mechanical Behavior and Design of Materials, Department of Precision Machinery and Instrumentation, University of Science and Technology of China, Hefei, Anhui 230027, China*

**Email:** [xuansh@ustc.edu.cn](mailto:xuansh@ustc.edu.cn) (SH XUAN), [gongxl@ustc.edu.cn](mailto:gongxl@ustc.edu.cn) (XL GONG)

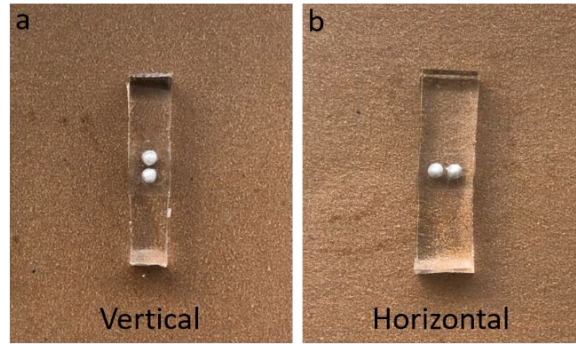


**Figure S1.** Optical photographs of the LMDE composites with (a) vertical and (b) horizontal arrangement of droplets.



**Figure S2.** (a) Optical photographs of different kinds of 3D printed molds and (b) the as-fabricated H-LMDE composites with different arrangement of droplets.

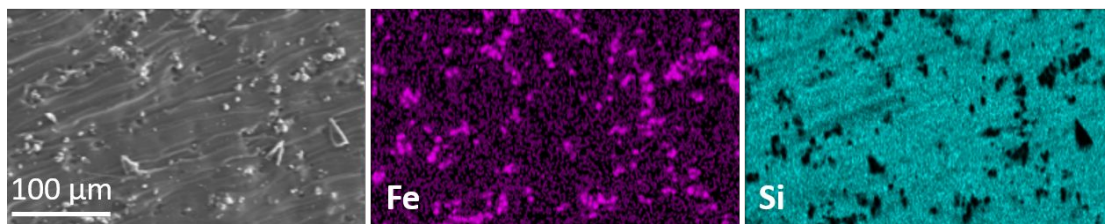


**Figure S3.** EDS mapping of the magnetic PDMS matrix for the as-fabricated H-LMDE composites.

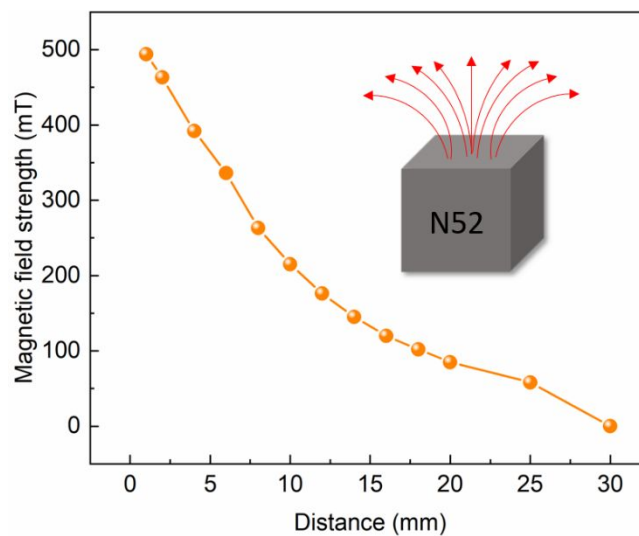


**Figure S4.** The magnetic field strength versus to the distance away from the surface of

N52 typed magnet.

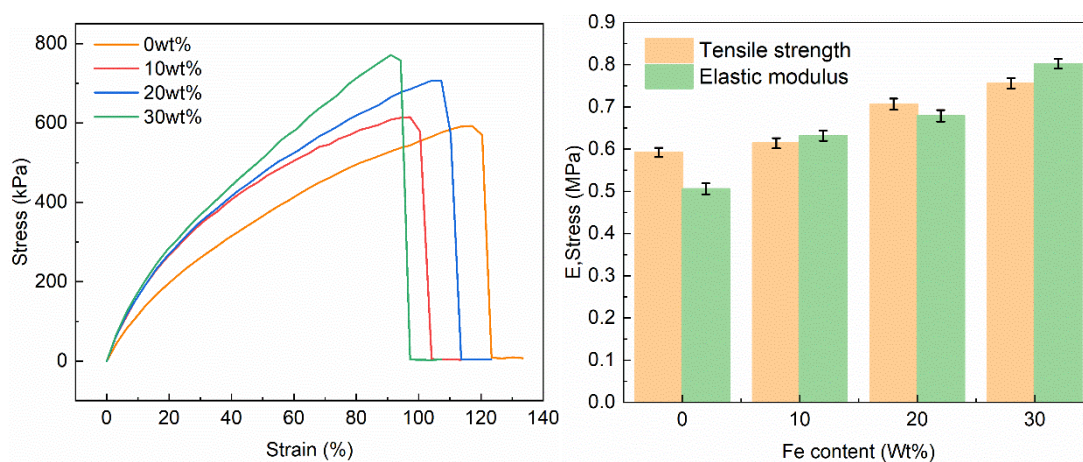


**Figure S5.** Tensile strength and elastic modulus of the elastomer matrix with different CIP contents.

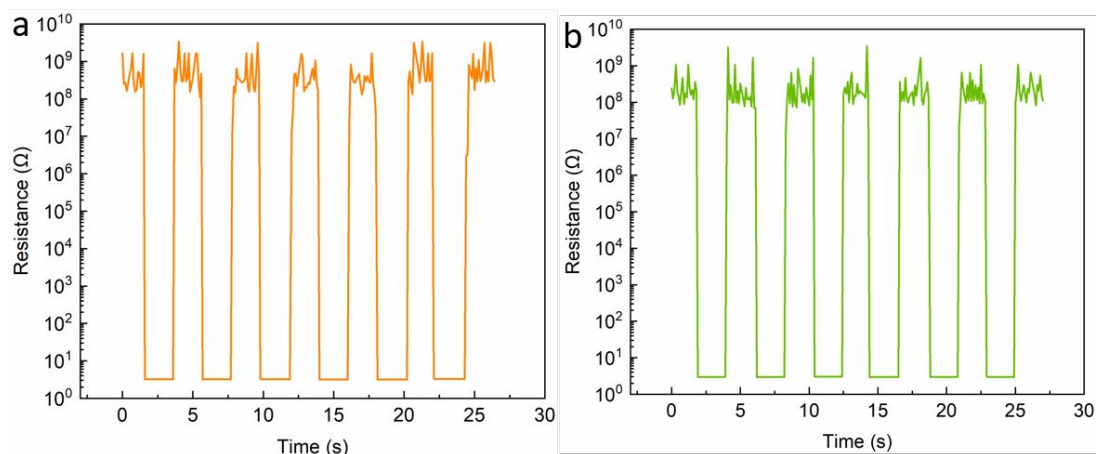


**Figure S6.** The corresponding resistance variation of the three (a) and four (b) LMDs embedded H-LMDE composite during cyclic stretching at 30 % strain.

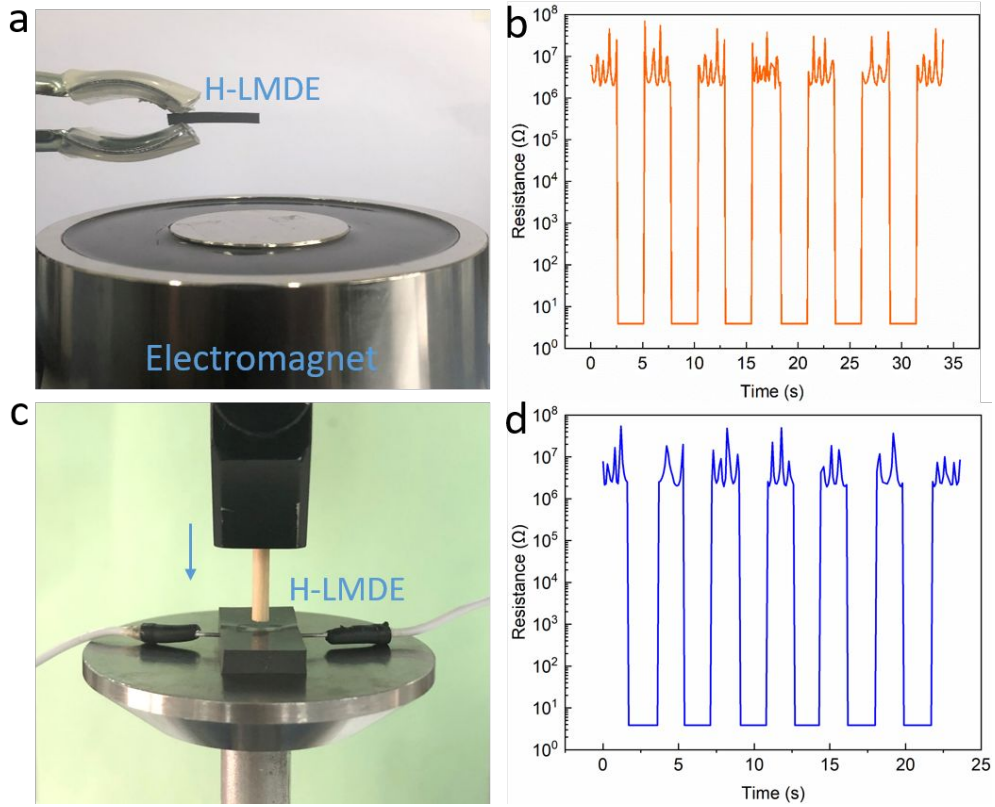


**Figure S7.** The digital images of test systems and corresponding resistance variation of the H-LMDE composite under cyclical magnetic field (a,b) and compression (c,d).

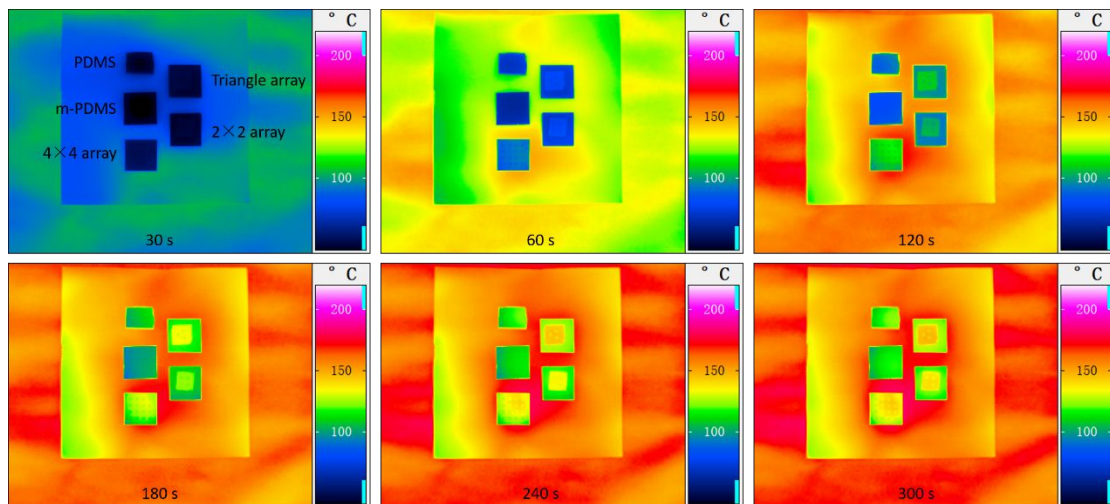


**Figure S8.** Infrared images of the surface temperature for different samples over time

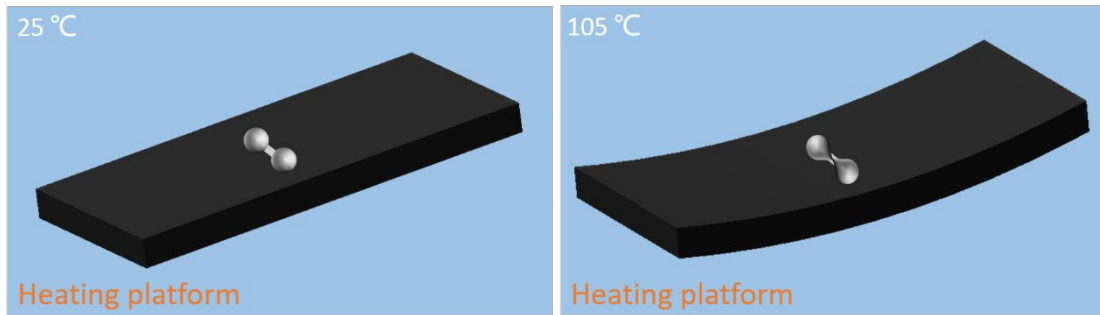


**Figure S9.** Schematic diagram of deformation of the H-LMDE composite during the heating process.

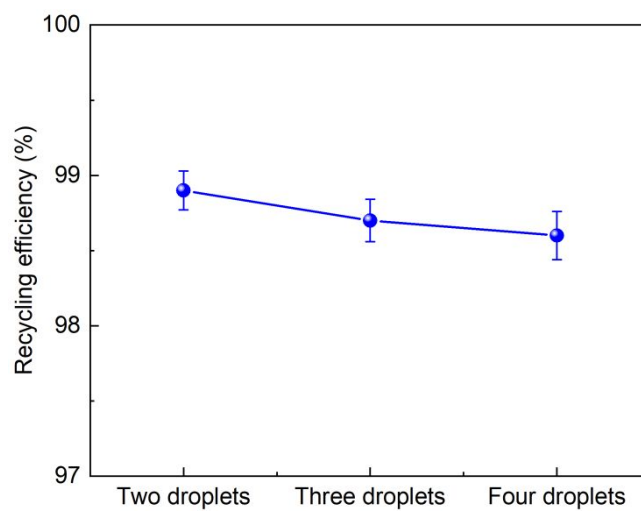


**Figure S10.** The recycling efficiency of the H-LMDE composites (30 wt% CIP content) with different numbers of LMDs.

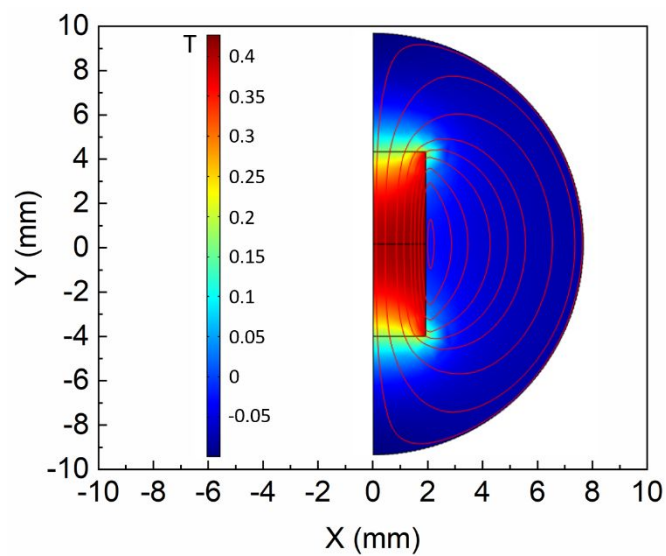


**Figure S11.** Magnetic field distribution of the NdFeB magnet.